

Alternate Learning based Sparse Semantic Communications for Visual Transmission

Siyu Tong, Xiaoxue Yu, Rongpeng Li, Kun Lu, Zhifeng Zhao, and Honggang Zhang

Abstract—Semantic communication (SemCom) demonstrates strong superiority over conventional bit-level accurate transmission, by only attempting to recover the essential semantic information of data. In this paper, in order to tackle the non-differentiability of channels, we propose an alternate learning based SemCom system for visual transmission, named SparseSBC. Specially, SparseSBC leverages two separate Deep Neural Network (DNN)-based models at the transmitter and receiver, respectively, and learns the encoding and decoding in an alternate manner, rather than the joint optimization in existing literature, so as to solving the non-differentiability in the channel. In particular, a “self-critic” training scheme is leveraged for stable training. Moreover, the DNN-based transmitter generates a sparse set of bits in deduced “semantic bases”, by further incorporating a binary quantization module on the basis of minimal detrimental effect to the semantic accuracy. Extensive simulation results validate that SparseSBC shows efficient and effective transmission performance under various channel conditions, and outperforms typical SemCom solutions.

Index Terms—Sparse semantic communication, visual transmission, alternate self-critic learning.

I. INTRODUCTION

RECENTLY, faced with the advent of the Internet of Intelligence (IoI) [1], semantic communications [2], [3], which put more emphasis on the semantic-level accuracy, emerge as a novel and promising solution and attract significant research interest, as the classical bit-level accuracy-oriented communication techniques approach the Shannon limit and fail to satisfy stringent requirements in the IoI era.

In line with implementation maturity to extract semantic features from the source, SemCom could be generally classified as text, speech, image and video transmission. For example, Long Short-Term Memory (LSTM) and Transformer [4]-based natural language processing techniques have been extensively leveraged to design a Joint Source-Channel Coding (JSCC) mechanism [5] for text transmission [6]–[8]. Meanwhile, in order to understand emotions and tunes of speech more thoroughly, attention-based squeeze-and-excitation [9] and symbol

recognition modules [10] have been added to the basic JSCC structure for speech transmission. Furthermore, as for image transmission, limited to the storage of equipment and capability of transmission channel, JSCC-based image transmission methods [11], [12] are often contingent on image compression works. In that regard, Convolutional Neural Network (CNN)-based [13], [14] and Recurrent Neural Network (RNN)-based methods [15] demonstrate astonishing performances in (lossy) image compression. Besides, a Generative Adversarial Network (GAN)-based method [16] achieves real-time adaptive compression. Belonging to the most challenging works, semantic video transmission takes account of the temporal relationship across frames and calibrates Deep Neural Networks (DNNs) to implement conditional coding and context learning, so as to capture essential keypoints and adapt to wireless channels [17], [18]. Notably, most works adopt an end-to-end approach to train Neural Network structures, and implicitly assume the differentiability in channel layer. Nevertheless, such an assumption might not hold in practice [2].

On the other hand, given the wide application of images and videos, extensive signal processing techniques are available to image and video compression. For example, JPEG and JPEG2000 utilize quantization and entropy coder to compress images for fewer-bits transmission. Meanwhile, HEVC [19] and MPEG adopt the hybrid coding framework based on transform coding and prediction. Furthermore, as a sub-Nyquist sampling framework, Compressive Sensing (CS) has been employed to capture the sparsity in images and boost the performance of numerous imaging applications [20]. Unfortunately, in the literature, there shed little light on explicitly investigating the sparsity into semantic image and video transmission. However, considering the successful applications of CS, it remains worthwhile to effectively combine latest sparsity-driven techniques and advanced DNNs towards SemCom on image and video transmission.

In this paper, we put forward SparseSBC, an alternate learning based sparse SemCom framework for image and video transmission. In particular, SparseSBC involves a transmitter and a receiver to learn the transmission scheme by turns, so as to be applicable for both differentiable and non-differentiable channel. In addition, SparseSBC adapts a “self-critic” scheme to overcome the divergence in training. Furthermore, SparseSBC deduces semantic bases which can describe all semantic embeddings with calibrated DNN-driven modules. On top of that, SparseSBC quantizes the sparsely represented bits from the space of semantic bases for transmission. Conversely,

This work was supported in part by the National Natural Science Foundation of China under Grants 62071425, in part by the Zhejiang Key Research and Development Plan under Grant 2022C01093, in part by Huawei Cooperation Project, and in part by the Zhejiang Provincial Natural Science Foundation of China under Grant LR23F010005.

S. Tong, X. Yu, and R. Li are with College of Information Science and Electronic Engineering, Zhejiang University (email: {tongsiyu, sdwhyx, lirongpeng}@zju.edu.cn).

K. Lu was with Zhejiang University and is now with Huawei Technologies Co., Ltd. (email: lukun199@zju.edu.cn).

Z. Zhao and H. Zhang are with Zhejiang Lab as well as Zhejiang University (email: {zhaozf, honggangzhang}@zhejianglab.com).

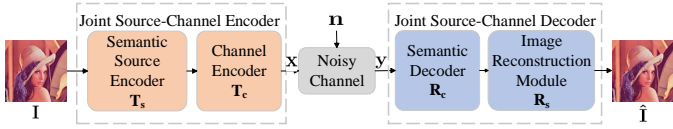


Fig. 1. Typical block structure of SemCom.

jointly taking account of sparse signal recovery and JSCC-based decoding, SparseSBC reconstructs the image from received noisy bits.

In brief, the major contribution of this work can be summarized as follows:

- We put forward SparseSBC, an alternate learning based sparse SemCom framework for image and video transmission, by effectively combining the concept of CS and the advance of DNNs. In particular, a “self-critic” scheme is introduced into the training procedure to achieve better exploration and stable process.
- Within SparseSBC, at the transmitter side, besides the encoder, we additionally transform semantically encoded bits into the space of semantic bases and quantize the results by building up DNN-driven non-linear mapping. Meanwhile, similar operations are applied to the receiver side as well.
- Through extensive simulations in various channel conditions, we validate that SparseSBC shows superior performance than JSCC and JPEG, in terms of the required transmission bits to obtain competitive reconstruction performance.

The remainder of the paper is organized as follows. In Section II, we present the framework of SparseSBC, while the details of SparseSBC for image and video transmission are shown in Section III. Section IV gives the corresponding simulation results. Section V concludes the paper.

II. SYSTEM MODEL

A. General Framework of SemCom

As illustrated in Fig. 1, we primarily consider the SemCom framework encompassing an encoder \mathcal{T} and a decoder \mathcal{R} as transmitter (TX) and receiver (RX) respectively, as well as a noisy channel \mathcal{H} . Both encoder and decoder are implemented by DNN and mutually contingent. Specifically, the encoder is logically comprised of two DNN-based modules (i.e., a semantic source encoder \mathbf{T}_s and a channel encoder \mathbf{T}_c) to extract low-dimensional features from the original image and encode them into symbols for channel transmission, respectively. Without loss of generality, an image \mathbf{I} , with $d_1 \times d_2$ pixels, can be downsampled to lower-dimension embeddings $\mathbf{x} \in \mathbb{R}^M$ as

$$\mathbf{x} = \mathbf{T}_c(\mathbf{T}_s(\mathbf{I})). \quad (1)$$

Notably, video transmission can be conveniently transformed to image transmission, as a video consists of a sequence of images [17], [18]. Therefore, as depicted in Fig. 7, after taking the first frame of image as the base background, subsequent images in a video can be obtained by further computing the difference of corresponding pixel’s value between the two

frames and taking the absolute values. This kind of differential images only record the moving parts in a video, and is easier to be compressed due to the inherent sparsity. Besides, in order to offset the accumulated effect of noise, we set a new frame as the latest background (i.e., the basis for differential operation) every 12 frames.

At the receiver side, the received signals \mathbf{y} can be formulated as $\mathbf{y} = \mathbf{h}\mathbf{x} + \mathbf{n}$, where \mathbf{h} denotes the channel coefficients, \mathbf{n} represents the independent and identically distributed (i.i.d.) noise in channel, following a circularly symmetric Gaussian distribution. In that regard, the channel could be modeled as a non-trainable layer to fit the training process. Typically, the Additive White Gaussian Noise (AWGN) channel and the Phase-Invariant Fading (PIF) channel are generally considered in most typical studies [2]. Mathematically, the channel can be considered as an AWGN channel when \mathbf{h} is set to $\mathbf{1}$, while in PIF channel \mathbf{h} is assumed to follow a constant distribution.

Conversely, RX utilizes a semantic channel decoder \mathbf{R}_c and an image reconstruction module \mathbf{R}_s to recover from noisy bits. Besides, with a denormalization layer, for every color channel each pixel’s value is restored to $(0, 255)$. Mathematically,

$$\hat{\mathbf{I}} = \mathbf{R}_s(\mathbf{R}_c(\mathbf{y})), \quad (2)$$

where $\hat{\mathbf{I}}$ denotes the reconstructed image. Basically, to further evaluate the quality of the reconstructed image, we adopt the L_1 -norm between pixels in the original image and reconstructed one. In other words, $\mathcal{L} = \frac{1}{2d_1d_2} \sum_{i,j}^{d_1,d_2} |\mathbf{I}_{i,j} - \hat{\mathbf{I}}_{i,j}|$, where $\mathbf{I}_{i,j}$ denotes the pixel (i, j) of a $d_1 \times d_2$ image \mathbf{I} . And the smaller \mathcal{L} yields higher semantic similarity of \mathbf{I} and $\hat{\mathbf{I}}$.

B. Framework of SparseSBC

Fig. 2 presents the framework of SparseSBC. Notably, compared to SemCom in Fig. 1, SparseSBC prominently adds a CS-consistent DNN module \mathbf{Q}_T to further map \mathbf{x} to $\hat{\mathbf{x}} \in \mathbb{Z}_2^N$, where $\mathbb{Z}_2 = \{0, 1\}$. Since each image can be fully described by semantic bases, through the process of \mathbf{Q}_T , an image can be expressed sparsely in terms of a specific set of bases, and thus transformed into a sequence of bits with larger compression ratio. Correspondingly,

$$\hat{\mathbf{x}} = \mathbf{Q}_T(\mathbf{x}) = \mathbf{Q}_T(\mathbf{T}_c(\mathbf{T}_s(\mathbf{I}))). \quad (3)$$

After receiving the sparse quantization signal $\hat{\mathbf{x}}$, RX uses another dequantization module \mathbf{Q}_R to process the received signal $\hat{\mathbf{y}} = \mathbf{h}\hat{\mathbf{x}} + \mathbf{n}$ and recover the images, that is,

$$\hat{\mathbf{I}} = \mathbf{R}_s(\mathbf{R}_c(\mathbf{Q}_R(\hat{\mathbf{y}}))). \quad (4)$$

In resemblance to CS [20], \mathbf{Q}_T and \mathbf{Q}_R is somewhat equivalent to nonlinear mapping and reconstruction matrices. Besides, for simplicity of representation, we denote the transmitter as $\mathcal{T} = \mathbf{Q}_T(\mathbf{T}_c(\mathbf{T}_s(\cdot)))$ and the receiver as $\mathcal{R} = \mathbf{R}_s(\mathbf{R}_c(\mathbf{Q}_R(\cdot)))$ hereafter.

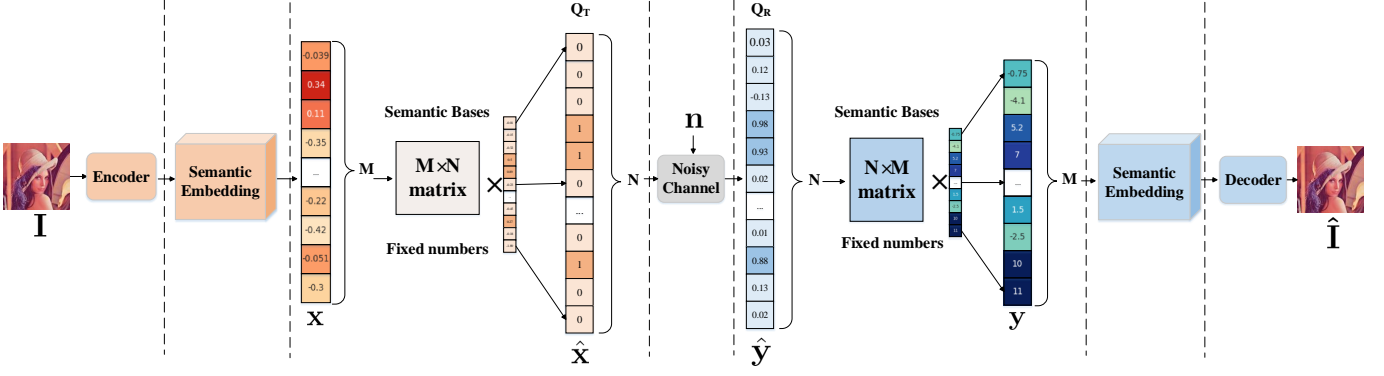


Fig. 2. Framework of SparseSBC.

Apart from adopting \mathcal{L} (i.e., L_1 -norm) to measure the semantic similarity, a sparse factor \mathcal{L}_s will be used to impose the sparsity of the transmitted bits. In other words,

$$\mathcal{L}_{\text{full}} = \underbrace{\frac{1}{2N} \sum_{i,j}^{d_1, d_2} |\mathbf{I}_{ij} - \hat{\mathbf{I}}_{ij}|}_{\mathcal{L}} + \varepsilon \underbrace{\sum_{i=1}^N |\hat{x}_i|}_{\mathcal{L}_s}, \quad (5)$$

where $\hat{\mathbf{x}} = [\hat{x}_1, \dots, \hat{x}_N]$ and ε denotes the sparsity weight.

Next, we will explain how to develop modules \mathbf{Q}_T and \mathbf{Q}_R , and use the distributed training scheme to bypass the differentiability issue of random channels.

III. IMPLEMENTATION DETAILS OF SPARSESBC

A. DNN Structure

In this paper, we adopt the following DNN structure and provide one viable means while leaving the utilization of other DNN structures (e.g., transformer [4]) as future works. Besides, we denote the parameters in the transmitter and receiver DNNs (i.e., \mathcal{T} and \mathcal{R}) as ϕ and θ , respectively.

1) Design of Source & Channel Encoder and Decoder

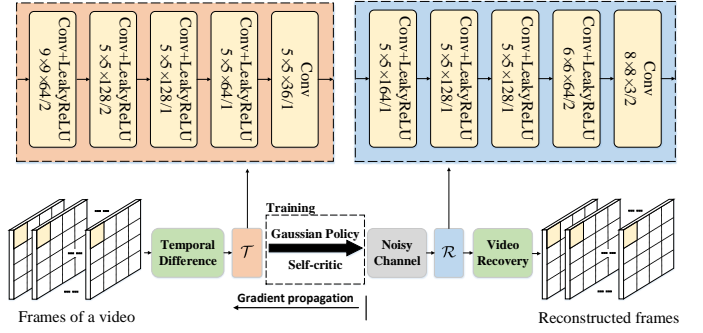
At the transmitter side, the joint encoder \mathcal{T} encompasses multiple convolutional layers with LeakyReLU activation functions to extract semantic features from an image \mathbf{I} and reshape to an M -length vector \mathbf{x} . Similarly, the decoder at the receiver side contains de-convolutional layers to restore the images.

2) Design of \mathbf{Q}_T and \mathbf{Q}_R

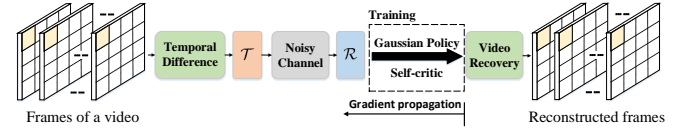
The DNN for both \mathbf{Q}_T and \mathbf{Q}_R consists of a fully connected layer with Tanh activation function, so as to transform semantically encoded bits to a sequence of numbers ranging from -1 to 1 . Afterwards, a binary quantization is performed to obtain an N -length binary bits vector (i.e., containing 0s or 1s only). Notably, such a fully connected layer resembles the mapping and reconstruction matrices (to map and reconstruct from semantic bases) in CS; while the latter Tanh function and quantization module capture non-linear transformations.

B. Alternate learning based SparseSBC

1) Integration of Alternate Learning and SemCom Most typical SemCom schemes discuss the differentiable objective optimization, but such a stringent assumption on transmission channels might not always hold in practice. Therefore, we



(a) The training phase of TX.



(b) The training phase of RX.

Fig. 3. The details of TX and RX in training period, which both adopt distributed training scheme.

consider an alternate learning scheme into SemCom to deal with the non-differentiability of random channels and help to turn the whole learning system into a collaborative semantic transceiver.

To better illustrate the details of alternate learning, we define the input of \mathcal{T} and \mathcal{R} as \mathbf{s} at time t respectively. That is, for the transmitter, it encodes $s_{\text{en}}^{(t)} = \mathbf{I}^{(t)} \in \mathbb{R}^{d_1 \times d_2}$ to $a_{\text{en}}^{(t)} = \hat{\mathbf{x}}^{(t)} \in \mathbb{Z}_2^N$, and at the receiver side, $s_{\text{de}}^{(t)} = \hat{\mathbf{y}}^{(t)} \in \mathbb{R}^N$ and $a_{\text{de}}^{(t)} = \hat{\mathbf{I}}^{(t)} \in \mathbb{R}^{d_1 \times d_2}$. Both the transmitter and the receiver target to reconstruct images as close as the original signals. Meanwhile, the transmitter shall impose the sparsity of encoded embeddings. Hence, for the transmitter parameterized by ϕ and the receiver parameterized by θ , the learning reward can be formulated as

$$r_{\phi}^{(t)} = \Theta_{\phi}(\mathbf{I}, \hat{\mathbf{I}}, \hat{\mathbf{x}}) = 1 - \mathcal{L}_{\text{full}}, \quad (6a)$$

$$r_{\theta}^{(t)} = \Theta_{\theta}(\mathbf{I}, \hat{\mathbf{I}}) = 1 - \mathcal{L}. \quad (6b)$$

Different from JSCC systems, in order to maximize the learning reward, we train the encoder and decoder alternately

by taking a batch of T samples (i.e., image transmissions) as a mini-batch to optimize the following objective function

$$J = \mathbb{E}_{a^{(1)}, \dots, a^{(T)}} \left[\sum_{t=1}^T r^{(t)} \right], \quad (7)$$

where r takes the formula in (6b) and (6a) for ϕ and θ , respectively.

2) *Training Procedures* In this part, we primarily introduce the training procedures of the transmitter in depth. As the terminology ‘‘alternate learning’’ implies, we freeze θ and thus the objective function is only parameterized on ϕ , that is, $J(\phi)$ and r_ϕ . To further overcome the difficulty of divergence in training for high-dimensional semantic space, inspired by the methodology in Reinforcement Learning (RL), we adopt a simpler and quicker scheme named ‘‘self-critic’’ [21] based on the Gaussian policy gradient. In particular, we attempt to learn an optimal policy ϕ^* for TX:

$$\phi^* = \arg \max_{\mathcal{T}} \Theta_\phi(\mathbf{I}, \underbrace{\mathcal{R}(\mathcal{H}(\mathcal{T}(\mathbf{I})))}_{\text{no grad}}). \quad (8)$$

Notably, instead of training the model to estimate the baseline directly, we use the average return from a group of parallel samples as the baseline [21]. Specifically, we repetitively generate the encoding results from the input $\mathbf{s}^{(t)}$ m times according to the Gaussian distribution.

$$\hat{\mathbf{x}}_i^{(t)} \sim \mathcal{S} \left(\mathcal{N} \left(\boldsymbol{\mu}_\phi^{(t)} = \hat{\mathbf{x}}^{(t)}, \boldsymbol{\Sigma} \right) \right), \forall i = \{1, \dots, m\}, \quad (9)$$

where \mathcal{S} denotes the parallel sampling following the Gaussian distribution \mathcal{N} . $\boldsymbol{\Sigma} = (\sigma^2 \mathbf{E}) \in \mathbb{R}^{N \times N}$ is a covariance matrix set by the identity matrix \mathbf{E} and a scale factor σ , which can be regarded as an exploration factor to get more abundant expression of embeddings. Since a constant σ may not be well realized for exploration and exploitation, we can adjust the value of σ in different stages of training procedure dynamically, similar with the simulated annealing algorithm, wherein the value of σ gradually decreases along with the increase of epoches (denoted as ‘‘Annealed’’). Furthermore, we also consider $\sigma = [\sigma_1, \dots, \sigma_N]$ to be a learnable vector (denoted as ‘‘Learnable’’), which can be determined by a sigmoid function of the encoded bits, that is, $\sigma_i = \text{Sigmoid}(\hat{\mathbf{x}}_i), i \in \{1, 2, \dots, N\}$.

Following the decoding operation at the receiver side, we can obtain m rewards, that is, $\Theta_i, i \in \{1, \dots, m\}$ taking a value Θ_ϕ . Without loss of generality, for any i , by regarding the average of the remaining $m-1$ outputs as the bias term, we calculate the difference between Θ_i and the bias term for its parameter update. On the other hand, following our previous work [22], we have the following theorem to demonstrate the result of the policy gradient propagation for TX.

Theorem 1: Let $\tilde{\mathcal{T}}(\mathbf{I})^{(t)}$ be one of the multi-sampled embeddings in TX at time t . With the self-critic Gaussian policy gradient defined in (9), the gradient propagation for TX is given as

$$\nabla_\phi \log \left(\pi_\phi^{(t)} \right) = \left[\tilde{\mathcal{T}}(\mathbf{I})^{(t)} - \mathcal{T}(\mathbf{I})^{(t)} \right]^\top \boldsymbol{\Sigma}^{-1} \left[\nabla_\theta \mathcal{T}(\mathbf{I})^{(t)} \right]. \quad (10)$$

Algorithm 1 Distributed training based SparseSBC

Input: Batch size $T = 64$, initial learning rate $\alpha = 1e^{-4}$, self-critic samples $m = 5$, epoch $E = 200$, semantic similarity metric Θ , scale factor σ

Output: Encoder parameter ϕ , decoder parameter θ

- 1: For video transmission: Repeat the temporal-difference processing to obtain the base image (every 12 frames) and differential images
 - 2: **for** epoch = 1 : E **do**
 - 3: **Training TX**
 - 4: For each batch, TX encodes each sample image into its sparse binary embedding, on the basis of frozen parameters θ at the RX.
 - 5: TX samples m random samples according to (9), and sends the encoded bitstreams through the channel.
 - 6: RX decodes with the semantic policy gradient (11), thus yielding the objective function (6a).
 - 7: TX takes gradient propagation towards ϕ , and updates ϕ with α (12).
 - 8: **Training RX**
 - 9: For each batch, TX encodes m image samples into its sparse binary embeddings, based on its trained policy.
 - 10: TX sends encoded bitstreams through the channel.
 - 11: RX samples a sequence of random symbols from channel with the Gaussian distribution, decodes and calculates the objective function (6b).
 - 12: RX updates θ with Gaussian policy.
 - 13: **end for**
 - 14: **return** the parameters $\langle \phi, \theta \rangle$
-

Therefore, the calculation of the semantic policy gradient can be summarized as

$$\nabla J(\phi) \approx \frac{1}{mT} \sum_{i=1}^m \left[\sum_{t=1}^T \nabla_\phi \log \pi_{i;\phi}^{(t)} \left(\Theta_i - \text{avg}_{k \sim m; k \neq i} (\Theta_k) \right) \right], \quad (11)$$

where $\text{avg}(\cdot)$ calculates the mean value. Finally, we update ϕ with a learning rate α , as

$$\phi \leftarrow \phi - \alpha \nabla J(\phi). \quad (12)$$

Notably, such a ‘‘self-critic’’ training scheme can alleviate the high variance problem of the plain policy gradient and keep a stable training procedure [21].

Similarly, in the training period of θ , ϕ is frozen as well and the Gaussian policy gradient-based ‘‘self-critic’’ is identically adopted to reconstruct images from received embeddings. Afterwards, the objective of RX can be optimized as

$$\theta^* = \arg \max_{\mathcal{R}} \Theta_\theta(\mathbf{I}, \underbrace{\mathcal{R}(\mathcal{H}(\mathcal{T}(\mathbf{I})))}_{\text{no grad}}). \quad (13)$$

We summarize the details of SparseSBC in Algorithm 1.

TABLE I
SIMULATION SETTINGS

Parameter	Value
Learning rate α	10^{-4}
Batch size T	64
Sparse weight ε	0.1
Length of $\tilde{\mathbf{x}}$ N	5000
Length of $\hat{\mathbf{y}}$ M	2304
Self-critic samples m	5
Scale factor σ	0.1
Image dataset	Cifar-10

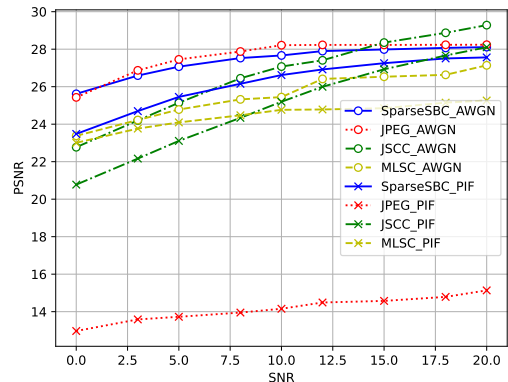
IV. SIMULATION RESULTS

In this section, we evaluate the performance of SparseSBC, and compare it with works like JSCC [11], Multi-Level Semantics-aware Communication system (MLSC) [14] and JPEG. In particular, we adopt the popular dataset Cifar-10 [23], which contains 60,000 RGB images, with fixed sizes of 32×32 , as well as a recorded video clip.

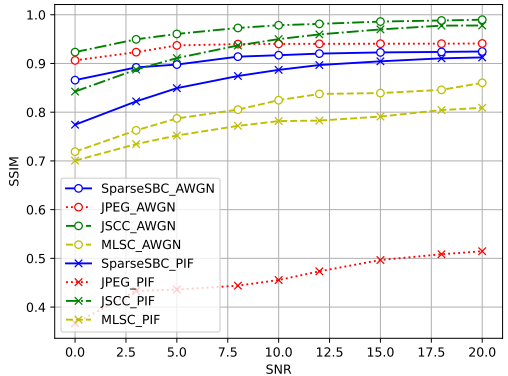
In addition, we evaluate the performance in terms of metrics like number of transmitted bits, Peak Signal-to-Noise Ratio (PSNR) [11], and Structural Similarity Index Measure (SSIM) [24]. These two metrics respectively evaluate the recovered images objectively and subjectively. In particular, PSNR measures the ratio between the maximum possible power of signal and noise which corrupts the signal, and can be defined as $10 \log_{10} \frac{\text{MAX}^2}{\text{MSE}} (dB)$, where $\text{MSE} = \frac{1}{d_1 d_2} \sum_{i,j}^{d_1, d_2} (\mathbf{I}_{i,j} - \hat{\mathbf{I}}_{i,j})^2$ denotes the mean squared-error, and MAX is the maximum value of pixels in the image of interest (i.e., 255 for 24-bit depth RGB images). On the other hand, SSIM, which is calculated as $\rho_l(\mathbf{I}, \hat{\mathbf{I}})^{\lambda_1} \cdot \rho_c(\mathbf{I}, \hat{\mathbf{I}})^{\lambda_2} \cdot \rho_s(\mathbf{I}, \hat{\mathbf{I}})^{\lambda_3} \in [0, 1]$, captures luminance, contrast and structural differences between images by ρ_l , ρ_c and ρ_s with exponential coefficients λ_1 , λ_2 and λ_3 . Typical experimental settings are summarized in Table I.

We first testify the performance of SparseSBC under different channel conditions and present the performance comparison with JPEG, JSCC and MLSC in terms of PSNR and SSIM in Fig. 4. It can be observed from Fig. 4, under AWGN channels, SparseSBC achieves similar performance compared to JPEG, while in PIF channels SparseSBC significantly outperforms JPEG. In other words, JPEG hardly works in harsh environments while SparseSBC retains the performance to resist poor channels. Meanwhile, SparseSBC yields superior PSNR than JSCC and obtains competitive SSIM as JSCC, which shows a stable performance under the influence of channel noise. Furthermore, SparseSBC leads to superior performance than MLSC, which further demonstrates its advantages.

On the other hand, Table II summarizes average number of transmitted bits under different techniques. It can be observed that SparseSBC compresses every Cifar image to the fixed 625 bytes. As a comparison, JSCC needs approximately 2,300 bytes to approach similar PSNR as SparseSBC, while JPEG consumes more than 643 bytes to transmit an image and requires significantly more bits along with increasing image complexity. Meanwhile, SparseSBC outperforms MLSC in both transmitted bits and performance. In a nutshell, SparseSBC is rather communication efficient.



(a) PSNR



(b) SSIM

Fig. 4. Performance comparison of SparseSBC with JPEG, JSCC and MLSC in terms of PSNR and SSIM.

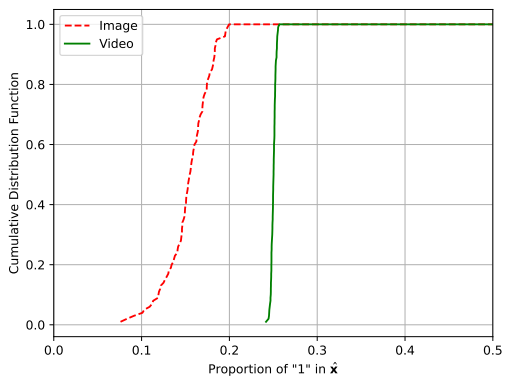


Fig. 5. The sparsity of transmitted bits in SparseSBC for image and video transmission.

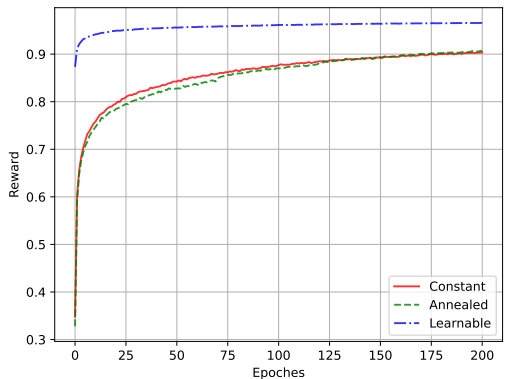


Fig. 6. The sensitivity the of scale factor σ .

TABLE II
COMPARISON OF SPARSESBC WITH THE TRADITIONAL DIGITAL METHOD JPEG AND GENERAL SEMCOM SYSTEM JSCC AND MLSC IN TERMS OF PERFORMANCE AND THE BITS OF ONE IMAGE TO BE TRANSMITTED (SNR=10).

	SparseSBC		General JSCC				MLSC-image	JPEG
Float Resolution (Bit)	1	1	4	8	16	32	32	1
No. Transmission Bytes	625	288	1,152	2,304	4,608	9,216	1,536	≥ 643
PSNR (dB)	27.66	13.18	19.40	27.13	27.16	27.16	25.44	28.21
SSIM (%)	92.12	60.79	84.43	97.67	97.83	97.83	80.46	94.37

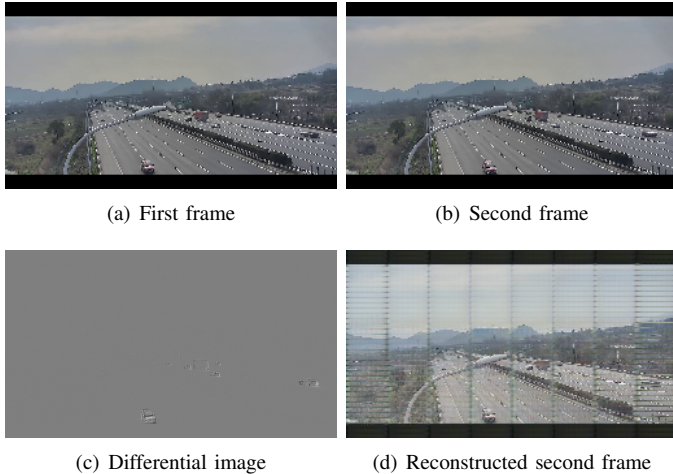


Fig. 7. Examples of differential images extracted by temporal difference from the video clip and reconstructed video frame.

Fig. 5 records transmitted bits for Cifar test images, and clearly demonstrates the sparsity of transmitted bits, since “1”s account for less than 20% of whole transmitted bits. Furthermore, similar observations apply for the video transmission with a sparsity of less than 30%. We also explore the sensitivity of the scale factor σ , as shown in Fig. 6. It can be observed that the learnable σ shows better performance in training period, which outperforms the constant and annealed value σ .

Fig. 7 illustrates the process of temporal difference for video transmission and presents the result to reconstruct the second frame based on temporal difference-involved SparseSBC. Though quantization and channel noise lead to performance reduction, SparseSBC shows its stable performance in video transmission.

V. CONCLUSIONS

In this paper, we have proposed a sparse SemCom system for visual transmission, named SparseSBC, which capably learns the DNN-based encoder and decoder deployed on the transmitter and receiver alternately, so as to adapt to the non-differentiable channel. In particular, a “self-critic” scheme has been leveraged into the training procedure to guarantee a stable process. In addition, by extracting a set of semantic bases and implementing binary quantization, semantic information is converted into sparse bitstreams, thus effectively bridging the potential combination between semantic communications and compressed sensing. Extensive simulation results validate that for visual transmission, SparseSBC outperforms JPEG and joint transmitter-receiver transmission schemes with efficiency and effectiveness under various channel conditions.

REFERENCES

- [1] R. Li *et al.*, “The collective advantage for advancing communications and intelligence,” *IEEE Wireless Commun.*, vol. 27, no. 4, pp. 96 – 102, Aug. 2020.
- [2] K. Lu *et al.*, “Rethinking modern communication from semantic coding to semantic communication,” *IEEE Wireless Commun.*, vol. 30, no. 1, pp. 158–164, 2023.
- [3] Z. Lu *et al.*, “Semantics-empowered communication: A tutorial-cum-survey,” *arXiv preprint arXiv:2212.08487*, Dec. 2022.
- [4] A. Vaswani *et al.*, “Attention is all you need,” in *Proc. NeurIPS*, Long Beach, CA, USA, Dec. 2017.
- [5] N. Farsad *et al.*, “Deep learning for joint source-channel coding of text,” in *Proc. ICASSP*, Calgary, AB, Canada, Apr. 2018.
- [6] H. Xie *et al.*, “Deep learning enabled semantic communication systems,” *IEEE Trans. Signal Proces.*, vol. 69, pp. 2663–2675, Mar. 2021.
- [7] —, “A lite distributed semantic communication system for Internet of things,” *IEEE J. Sel. Area. Comm.*, vol. 39, no. 1, pp. 142–153, Nov. 2020.
- [8] Q. Zhou *et al.*, “Semantic communication with adaptive universal transformer,” *IEEE Wirel. Commun. Lett.*, vol. 11, no. 3, pp. 453–457, Dec. 2021.
- [9] Z. Weng *et al.*, “Semantic communication systems for speech transmission,” *IEEE J. Sel. Area. Comm.*, vol. 39, no. 8, pp. 2434–2444, Jun. 2021.
- [10] G. Shi *et al.*, “A new communication paradigm: From bit accuracy to semantic fidelity,” *Chinese Journal on Internet of Things*, Jan. 2021.
- [11] E. Boursoulatzé *et al.*, “Deep joint source-channel coding for wireless image transmission,” *IEEE Trans. on Cogn. Commun. Netw.*, vol. 5, no. 3, pp. 567–579, May 2019.
- [12] D. B. Kurka *et al.*, “Bandwidth-agile image transmission with deep joint source-channel coding,” *IEEE Trans. Wirel. Commun.*, vol. 20, no. 12, pp. 8081–8095, Dec. 2021.
- [13] A. Prakash *et al.*, “Semantic perceptual image compression using deep convolutional networks,” in *Proc. DCC*, Snowbird, Utah, USA, Apr. 2017.
- [14] Z. Zhang *et al.*, “Wireless transmission of images with the assistance of multi-level semantic information,” in *Proc. ISWCS*, Hangzhou, Zhejiang, China, Oct. 2022.
- [15] G. Toderici *et al.*, “Full resolution image compression with recurrent neural networks,” in *Proc. CVPR*, Honolulu, HI, USA, Jul. 2017.
- [16] O. Rippel *et al.*, “Real-time adaptive image compression,” in *Proc. ICML*, Sydney, NSW, Australia, Aug. 2017.
- [17] P. Jiang *et al.*, “Wireless semantic communications for video conferencing,” *IEEE J. Sel. Area. Comm.*, vol. 41, no. 1, pp. 230–244, Jan. 2023.
- [18] S. Wang *et al.*, “Wireless deep video semantic transmission,” *IEEE J. Sel. Area. Comm.*, vol. 41, no. 1, pp. 214–229, Jan. 2023.
- [19] G. J. Sullivan *et al.*, “Overview of the high efficiency video coding (HEVC) standard,” *IEEE Trans. Circuits Syst. Video Technol.*, vol. 22, no. 12, pp. 1649–1668, Dec. 2012.
- [20] V. Kravets *et al.*, “Progressive compressive sensing of large images with multiscale deep learning reconstruction,” *Sci. Rep.*, vol. 12, no. 1, p. 7228, May 2022.
- [21] S. J. Rennie *et al.*, “Self-critical sequence training for image captioning,” in *Proc. CVPR*, Honolulu, HI, USA, Jul. 2017.
- [22] K. Lu *et al.*, “Reinforcement learning-powered semantic communication via semantic similarity,” *arXiv preprint arXiv:2108.12121*, Aug. 2021.
- [23] A. Krizhevsky *et al.*, “Learning multiple layers of features from tiny images,” *Handb. Syst. Autoimmune Dis.*, vol. 1, no. 4, Apr. 2009.
- [24] U. Sara *et al.*, “Image quality assessment through FSIM, SSIM, MSE and PSNR—A comparative study,” *J. Comput. and Commun.*, vol. 7, no. 3, pp. 8–18, Mar. 2019.